A Wideband Isotropic Radiated Planar Antenna Using Sequential Rotated L-Shaped Monopoles

Changjiang Deng, Yue Li, Zhijun Zhang, and Zhenghe Feng

***Abstract*—In this communication, we have proposed a compact planar antenna for isotropic radiation pattern in a wide operating band. The proposed antenna consists of four sequential rotated L-shaped monopoles that are fed by a compact uniform sequential-phase (SP) feeding network with equal amplitude and incremental 90° phase delay. Based on the rotated field method, a full spatial coverage with gain deviation less than 6 dB is achieved in a wide operating band from 2.3 to 2.61 GHz, also with well-impedance matching. A prototype of the proposed antenna has been built and tested. The measured results, including the reflection coefficient, gain, and radiation patterns, are analyzed and compared with the simulated results.**

***Index Terms*—Isotropic radiation pattern, rotated field, rotated sequential feeding network, wideband antenna.**

I. Introduction

With the rapid development of wireless communication, antennas with a quasi-isotropic radiation pattern are desired in many applications, especially in radio frequency identification (RFID) tags, wireless access points (APs) and aerospace applications. Such type of antenna has the merit of full spatial coverage, which is important for a reliable wireless communication system.

Isotropic antennas that radiate uniformly in every direction and polarization do not exist [1], however, quasi-isotropic radiation pattern, which has uniform power over a sphere in the far zone is possible [2]. Various types of antenna have been designed for quasi-isotropic radiation pattern. Tridimensional antenna is one attractive candidate [3]–[5]. For example, in [3], the combination of a monopole antenna and two slot antennas can provide a relatively isotropic radiation pattern. A method similar to [3] is used in [4], which consists of two tablets in the mold of a whistle. In [5], an electrical small spherical antenna with quasi-isotropic radiation pattern is proposed for wireless sensor networks. Besides single element, array antennas are also developed for full spatial coverage [6]–[8]. However, the geometry of these antenna designs is complicated and occupies a large space.

Planar antennas with quasi-isotropic radiation pattern have been proposed in [9]–[12] for low profile, low cost and easy fabrication. By combining a dipole mode and a loop mode [9], a pair of crossed electric and magnetic dipoles [10] or two crossed curved dipoles [11], an isotropic radiation pattern is produced with a single layer. In all these designs, the relative 6 dB gain deviation [12] bandwidth is normally around 3% or less. In [12], a very thin passive RFID tag antenna using two bent dipoles for quasi-isotropic radiation pattern is proposed. The 6 dB gain deviation bandwidth achieves 6.6%. However, this type of antenna does not work efficiently when mounted on a metallic object [13].

In [14], a compact sequential-phase (SP) feeding network is presented with equal amplitude and phases of 0°, 90°, 180°, and 270° in a wide bandwidth. In this communication, the SP feeding network is adopted to feed four L-shaped monopoles for quasi-isotropic radiation pattern. By arranging the four L-shaped monopoles in a rotationally symmetrical structure, complete full spatial coverage could be achieved in a wide bandwidth, which is the most important contribution of this communication.

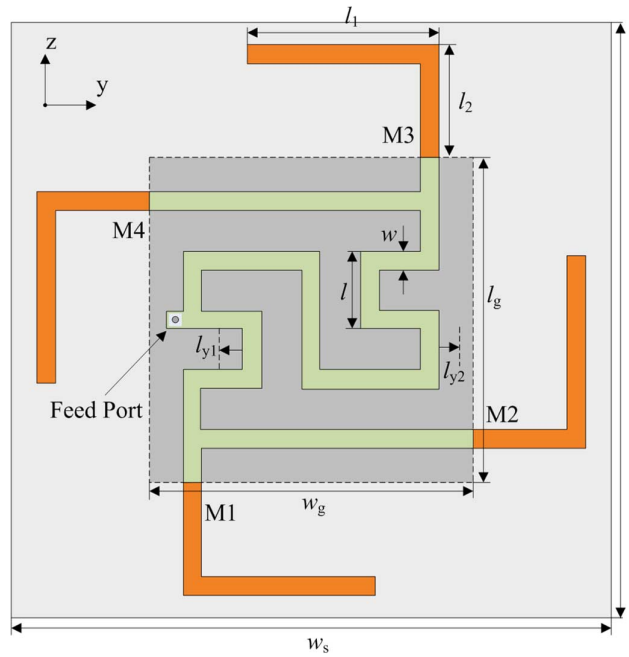

Fig. 1. Geometry of the proposed antenna structure.

II. Antenna Design

The geometry of the proposed antenna is shown in Fig. 1, which is fabricated with a layer of FR4 substrate ($h = 0.8$ mm, $\varepsilon = 4.4$, $\tan\delta = 0.02$). An SP feeding network and a ground plane are printed on the two sides of the substrate. The width of the microstrip line is designed to match 50-Ohm impedance. According to [14], the unit length of meander lines is $\lambda/16$ and the two meander lines have total lengths of $\lambda/4$ and $3\lambda/4$, providing an extra 180° phase difference and performing $\lambda/4$ impedance transformation. Thus, the SP feeding network provides four feed ports with equal amplitude and phases of 0°, 90°, 180°, and 270°. Four L-shaped monopoles, named as M1, M2, M3, M4, are arranged in rotational sequence, and connected to the corresponding feeding ports.

The operating principle of the proposed antenna for isotropic radiation pattern is illustrated in Fig. 2. Fig. 2(a) shows the sketch of the four L-shaped monopoles that are fed with different feeding combinations. In Fig. 2(b), M1 and M3 are excited with equal amplitude and 180° phase difference, while M2 and M4 are not excited. The radiation pattern is similar to that of a dipole and the null is at $\theta = 30°$. Similar radiation pattern can be seen in Fig. 2(c), where only M2 and

Manuscript received July 19, 2013; revised October 23, 2013; accepted November 29, 2013. Date of publication December 05, 2013; date of current version February 27, 2014. This work was supported in part by the National Basic Research Program of China under Contract 2013CB329002, in part by the National High Technology Research and Development Program of China (863 Program) under Contract 2011AA010202, the National Natural Science Foundation of China under Contract 61301001, the National Science and Technology Major Project of the Ministry of Science and Technology of China 2013ZX03003008-002, and the China Postdoctoral Science Foundation funded project 2013M530046.

The authors are with State Key Laboratory on Microwave and Digital Communications, Tsinghua National Laboratory for Information Science and Technology, Department of Electronic Engineering, Tsinghua University, Beijing 100084, China (e-mail: hardy_723@163.com).

Color versions of one or more of the figures in this communication are available online at http://ieeexplore.ieee.org.

Digital Object Identifier 10.1109/TAP.2013.2293787

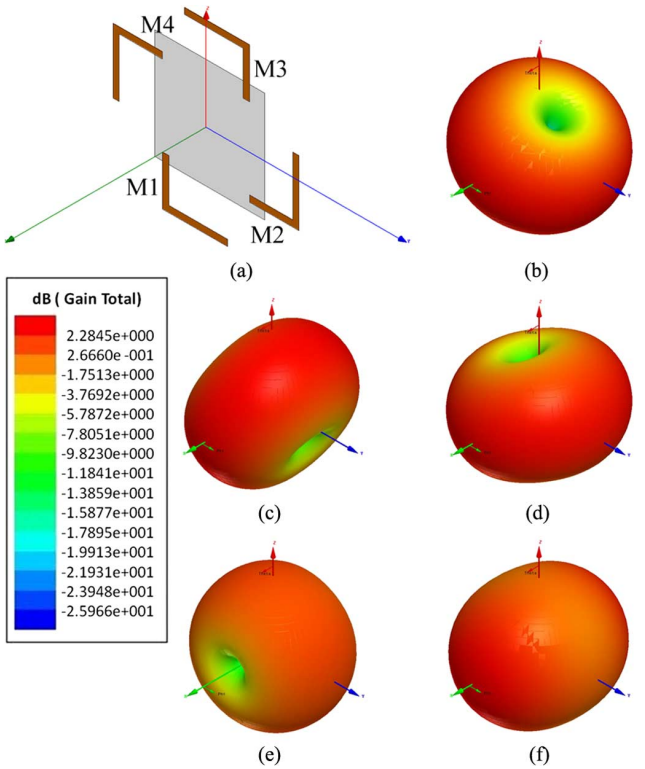

Fig. 2. (a) Sketch of four L-shaped monopoles; (b) only M1 and M3 are excited with equal amplitude and 180° phase difference; (c) only M2 and M4 are excited with equal amplitudes and 180° phase difference; (d) M1, M2, M3, M4 are excited with equal amplitude and phases differences of 0°, 0°, 180°, 180°; (e) M1, M2, M3, M4 are excited with equal amplitude and phases; (f) M1, M2, M3, M4 are excited with equal amplitude and sequential phases of 0°, 90°, 180°, 270°.

M4 operate, except that the null is at $\theta = 120°$. Thus, when the four monopoles are excited with equal amplitude and phases of 0°, 0°, 180°, and 180°, the radiation pattern is shown in Fig. 2(d), except that the null is at $\theta = 160°$. In Fig. 2(e), the four monopoles are excited with the same amplitude and phase. The nulls are still existed and along x-axis. However, when the four monopoles are fed with equal amplitude and a successive phase delay of 90° from element to element, an isotropic radiation pattern without nulls can be achieved, as shown in Fig. 2(f). In order to provide the sequential phase of 0°, 90°, 180°, and 270° in a wide bandwidth, the SP feeding structure in [14] are adopted and optimized with four L-shaped monopoles. For the antenna dimension consideration, the four monopoles are bent with L-shape. The compact SP feeding network adopted here is only about $\lambda/4 \times \lambda/4$. As there is mutual coupling between microstrip lines, the four feeding ports are not exactly with equal amplitude and phases of 0°, 90°, 180°, and 270°. Thus, some optimal tuning is needed to compensate for the coupling effects in the SP feeding network. That is, the shorter meander line is shortened by l_{y1} and the longer meander line is lengthened by l_{y2}, as is shown in Fig. 1. High Frequency Structure Simulator (HFSS) software is used to optimize the proposed antenna. These four monopoles are designed to operate at 2.4 GHz. The detailed values of each parameter are optimized and listed in Table I. There are several ways to evaluate the isotropic performance of an antenna. One typical method is to evaluate the sum of the squares of the electric fields with two polarizations. A criterion based on this method is proposed in [12], which is in the form of 6 dB gain deviation for an arbitrary angle. In this communication, the criterion is adopted to evaluate the spatial coverage performance of the proposed antenna.

TABLE I
DETAILED DIMENSIONS (UNIT: mm)

l_g	w_g	l_s	w_s	l
24.5	24.5	45	45	4.5
w	l_1	l_2	l_{y1}	l_{y2}
1.4	14.5	8.5	1	1

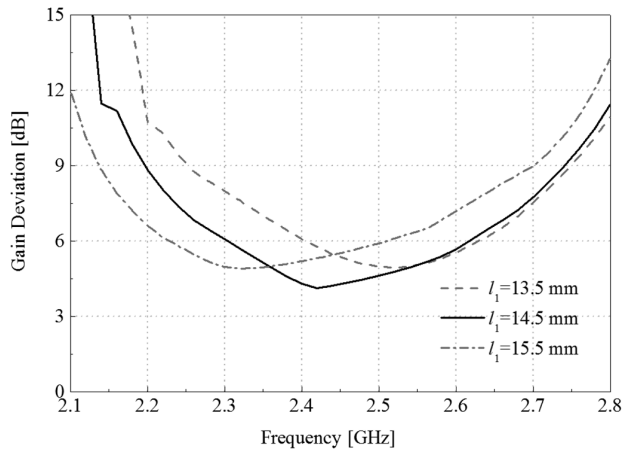

Fig. 3. Gain deviation with different l_1.

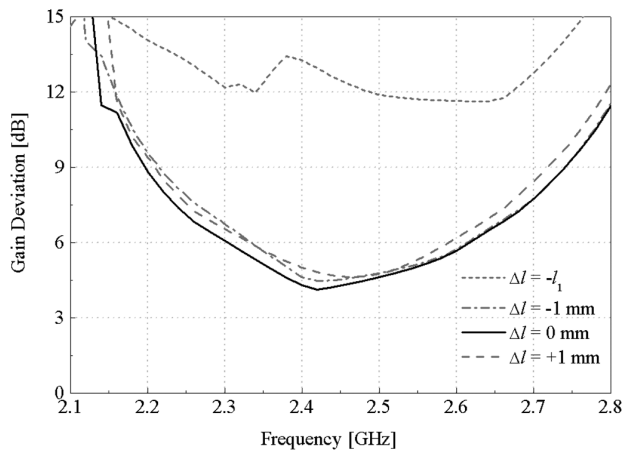

Fig. 4. Gain deviation with different Δl.

Fig. 3 shows the effect of l_1 on gain deviation of the proposed antenna. From the simulated results, it is observed that the resonant frequency becomes lower as l_1 increases. The widest 6 dB gain deviation bandwidth is achieved when l_1 is 14.5 mm. Similar results can be observed when varying l_2, which is the length of the other segment of the L-shaped monopole.

We also can tune the length difference between two arms for 6 dB gain deviation bandwidth optimization. We define $2 \times \Delta l$ as the length difference between the two monopole arms. Therefore, the lengths of two arms are $l_1 + \Delta l$, and $l_2 - \Delta l$. Selecting $l_1 = 14.5$ mm and $l_2 = 8.5$ mm, Fig. 4 shows the effect of Δl on 6 dB gain deviation bandwidth. The curves show that the gain deviation can be fine tuned by varying the value of Δl, while keeping the resonant frequency almost unchanged. When $\Delta l = -l_1$ (the four monopoles are straight), the gain deviation becomes worse. This difference may be explained that the two segments of L-arm can compensate the null in radiation pattern of each other. Thus, by tuning l_1 and Δl, optimized gain deviation bandwidth can be achieved.

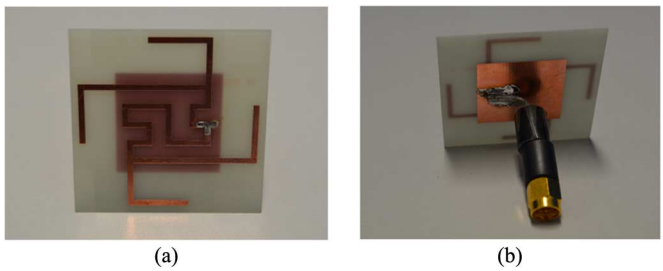

Fig. 5. Photograph of the fabricated antenna. (a) front view; (b) back view.

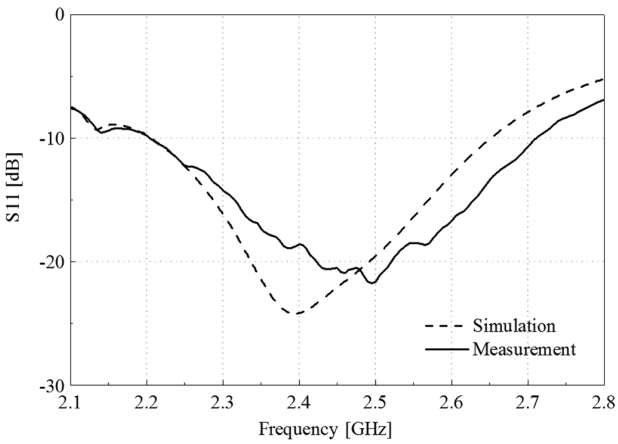

Fig. 6. Simulated and measured S_{11}.

III. Measurement Results

A prototype of the proposed antenna is fabricated and shown in Fig. 5 to validate the design. As the current in the feeding coaxial cable will disturb the electromagnetic field of the proposed antenna, some ferrite rings are used. Fig. 6 shows the measured reflection coefficient of the proposed antenna, which agrees well with the simulated result. The measured −10 dB reflection coefficient bandwidth is 510 MHz (2.2–2.71 GHz), or 20.82% corresponding to the center frequency of 2.45 GHz. In Fig. 7, we compare the measured and simulated gain deviation. It can be observed that the measured result is a little worse than the simulated result. This difference mainly comes from fabrication error, also with measurement error in the anechoic chamber. Besides, feeding cable can also perturb the radiation pattern during measurement process. The measured 6 gain deviation bandwidth is about 170 MHz (2.36–2.53 GHz), or 6.94% corresponding to the center frequency of 2.45 GHz.

Fig. 8 shows the normalized gain contour lines at 2.45 GHz. Owing to the symmetry of the proposed antenna, the θ angle is only plotted from 0° to 180°. The difference between the maximum and the minimum of gain is about 5.75 dB and it is smaller than 5 dB over 90% of the full space. It illustrates that the proposed antenna has an isotropic radiation pattern over the full space. Fig. 9 shows the simulated and measured results. The measured gain is higher than the simulated one. That is because the isotropic coverage of the fabricated antenna is worse than the ideal one in the simulation, considering the fabricated and measured error factors mentioned before. Therefore, the directivity of measurement is higher than the simulated one and peak gain is measured at 2.35 GHz. This effect can also be evaluated from the results in Fig. 7. However, the measured results are acceptable for isotropic radiation coverage in a wide bandwidth. The simulated radiation efficiency is also listed in Table II and is about 80% in the concerned band.

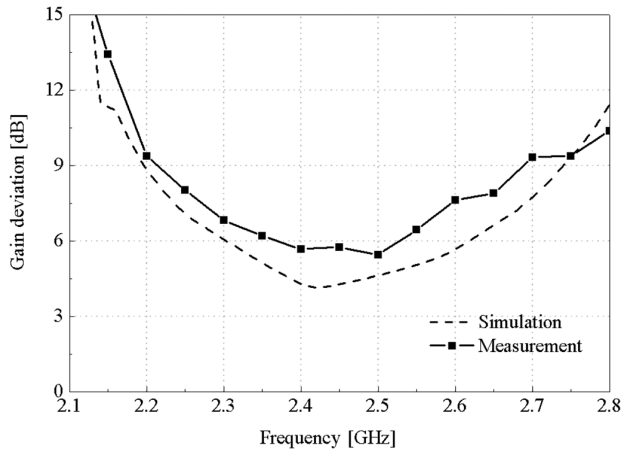

Fig. 7. Simulated and measured gain deviation.

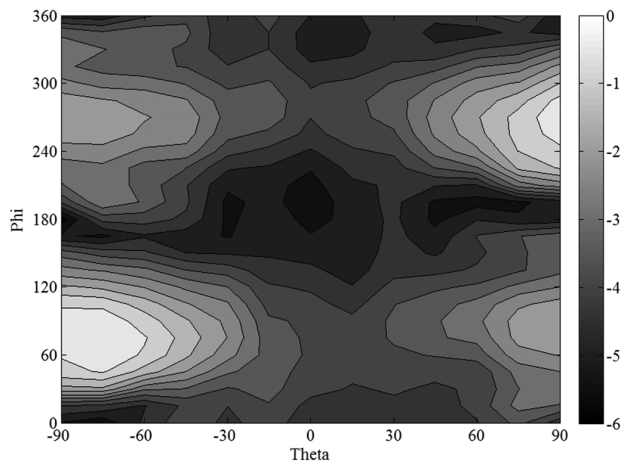

Fig. 8. Normalized gain contour lines at 2.45 GHz.

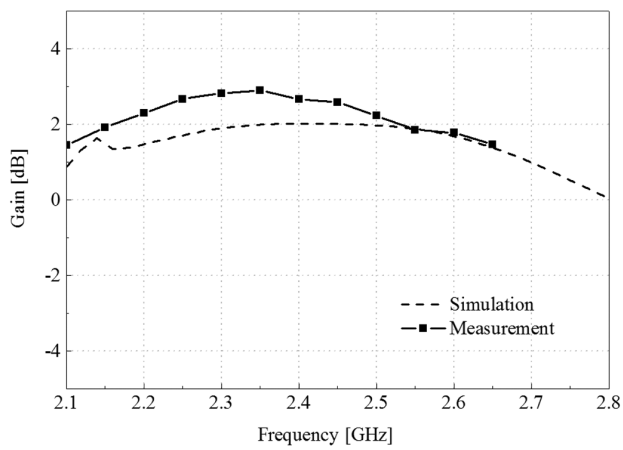

Fig. 9. Simulated and measured gain.

TABLE II
Simulated Radiation Efficiency

Frequency (GHz)	2.3	2.4	2.45	2.5	2.6
Efficiency (%)	84	83	82	81	77

IV. Conclusion

A compact planar antenna for isotropic coverage over the full space is presented in this communication. Four L-shaped monopoles are arranged in a rotationally symmetrical sequence and fed by an SP feeding network with equal amplitude and incremental 90° phase delay. The operating principle of the proposed antenna for isotropic radiation pattern is illustrated and experimentally verified. Compared with traditional isotropic radiated antenna, the proposed antenna achieves full spatial coverage in a much wider bandwidth, which is the most important contribution for this communication. The measured results show that the measured 6 dB gain deviation bandwidth is wider than 6.9%, which is within the −10 dB reflection coefficient bandwidth. Therefore, the proposed antenna is a promising candidate for achieving a full spatial coverage in a broad bandwidth.

References

[1] H. F. Mathis, "A short proof that an isotropic antenna is impossible," *Proc. IRE*, vol. 39, p. 970, 1951.

[2] H. Matzner and K. T. McDonald, Isotropic Radiators, Dec. 3, 2003 [Online]. Available: http://arxiv.org/pdf/physics/0312023.pdf, [physics class-ph]

[3] S. A. Long, "A combination of linear and slot antennas for quasi-isotropic coverage," *IEEE Trans. Antennas Propag.*, vol. 23, no. 4, pp. 572–576, Jul. 1975.

[4] E. S. Pires, G. Fontgalland, M. A. B. de Melo, R. M. Valle, G. F. Aragao, and T. P. Vuong, "A new quasi-isotropic antenna for ultra-wideband application," in *Proc. SBMO/IEEE MTT-S IMOC*, 2007, pp. 100–103.

[5] A. Mehdipour, H. Aliakbarian, and J. Rashed-Mohassel, "A novel electrically small spherical wire antenna with almost isotropic radiation pattern," *IEEE Antennas Wireless Propag. Lett.*, vol. 7, pp. 396–399, 2008.

[6] Z. Zhang, X. Gao, W. Chen, Z. Feng, and M. F. Iskander, "Study of conformal switchable antenna system on cylindrical surface for isotropic coverage," *IEEE Trans. Antennas Propag.*, vol. 59, no. 3, pp. 776–773, Mar. 2011.

[7] Psychogiou, Dimitra, and J. Hesselbarth, "Diversity antennas for isotropic coverage," in *Proc. Wireless Technology Conf. (EuWIT)*, 2010, pp. 101–104.

[8] H. Gazzah, "Optimum antenna arrays for isotropic direction finding," *IEEE Trans. Aerosp. Electron. Syst.*, vol. 47, no. 2, pp. 1482–1489, Apr. 2011.

[9] X. J. Xu, H. C. Huang, and Y. E. Wang, "Isotropic radiation from an electrically small loop-loaded printed dipole," in *Proc. IWAT*, Los Angeles, CA, USA, Mar. 2009, pp. 1–4.

[10] L. Liang and S. V. Hum, "A low-profile antenna with quasi-isotropic pattern for UHF RFID applications," *IEEE Antennas Wireless Propag. Lett.*, vol. 12, pp. 210–213, 2013.

[11] G. Pan, Y. Li, Z. Zhang, and Z. Feng, "Isotropic radiation from a compact planar antenna using two crossed dipoles," *IEEE Antennas Wireless Propag. Lett.*, vol. 11, pp. 1338–1341, 2012.

[12] C. Cho, H. Choo, and I. Park, "Broadband RFID tag antenna with quasi-isotropic radiation pattern," *Electron. Lett.*, vol. 41, no. 20, pp. 1091–1092, 2005.

[13] H. D. Chen and Y. H. Tsao, "Low-profile PIFA array antennas for UHF band RFID tags mountable on metallic objects," *IEEE Trans. Antennas Propag.*, vol. 58, no. 4, pp. 1087–1092, Apr. 2010.

[14] S. Lin and Y. Lin, "A compact sequential-phase feed using uniform transmission lines for circularly polarized sequential-rotation arrays," *IEEE Trans. Antennas Propag.*, vol. 59, no. 7, pp. 2721–2724, 2011.

The Effects of Spatial Dispersion on Power Flow Along a Printed-Circuit Tensor Impedance Surface

Amit M. Patel and Anthony Grbic

***Abstract*—In this communication, expressions for the group velocity and the direction of power flow along an idealized tensor impedance boundary condition (TIBC) and a printed-circuit tensor impedance surface (PCTIS), are found. A PCTIS consists of a patterned metallic cladding over a grounded dielectric substrate. The patterned metallic cladding is modeled by a tensor impedance sheet. Expressions for the surface impedance of a TIBC and a PCTIS are reviewed. From these expressions, the group velocity and direction of power flow are derived as a function of transverse wave vector. A PCTIS exhibits spatial dispersion due to the electrical thickness of its substrate while a TIBC does not. As a result of this spatial dispersion, a PCTIS can have the same surface impedance as a TIBC for a given transverse wave vector, but a different direction of power flow. The expressions for direction of power flow along a TIBC and a PCTIS are verified with a full-wave electromagnetic solver.**

***Index Terms*—Anisotropic structures, impedance sheets, metasurfaces, spatial dispersion, surface impedance, surface waves, tensor surfaces.**

I. Introduction

Electromagnetic metasurfaces are two-dimensional equivalents of volumetric metamaterials [1]–[4]. In metasurfaces, small inclusions (scatterers or apertures) are arranged along a surface with subwavelength spacing [5]. As a result, metasurfaces can be homogenized and macroscopically characterized by their effective polarizabilties or surface impedance instead of material parameters: μ and ϵ.

The demand for conformal and low profile waveguiding structures and antennas has led to increased interest in impedance surfaces. Various microwave devices have been devised by tailoring the scalar surface impedance profile of inhomogeneous surfaces [6]–[12]. Furthermore, tensor impedance surfaces (TISs), which were first studied analytically by Bilow [13], have been used to design devices such as polarization controlling antennas [14] and waveguiding surfaces [15]–[17]. These TISs are modeled using a single tensor impedance boundary condition (TIBC), which is given by

$$\begin{pmatrix} E_x \\ E_y \end{pmatrix} = \begin{pmatrix} \eta_{xx} & \eta_{xy} \\ \eta_{yx} & \eta_{yy} \end{pmatrix} \begin{pmatrix} -H_y \\ H_x \end{pmatrix} \tag{1}$$

Manuscript received April 29, 2013; revised October 09, 2013; accepted November 29, 2013. Date of publication December 05, 2013; date of current version February 27, 2014. This work was supported in part by a Presidential Early Career Award for Scientists and Engineers (FA9550-09-1-0696), an NSF Faculty Early Career Development Award (ECCS-0747623), and in part by the Science, Mathematics and Research for Transformation (S.M.A.R.T.) Fellowship sponsored by the U.S. Department of Defense (DoD) and the American Society for Engineering Education (ASEE).

A. M. Patel was with the Radiation Laboratory in the Department of Electrical Engineering and Computer Science at the University of Michigan, Ann Arbor, 48109 USA. He is now with the Applied Electromagnetics Lab, HRL Laboratories LLC, Malibu, CA 90265 USA (e-mail: amitmp@umich.edu).

A. Grbic is with the Radiation Laboratory in the Department of Electrical Engineering and Computer Science at the University of Michigan, Ann Arbor, 48109 USA (e-mail: agrbic@umich.edu).

Color versions of one or more of the figures in this communication are available online at http://ieeexplore.ieee.org.

Digital Object Identifier 10.1109/TAP.2013.2294196